Inhibition of MicroRNA-122-5p Relieves Myocardial Ischemia-Reperfusion Injury via SOCS1

Jun Zhang[1] Li Fu[1] Jing Zhang[1] Bo Zhou[1] Yanrong Tang[1] Zhenzhen Zhang[1] Tongqing Gu[2]

[1] Department of Cardiology, Chengdu First People's Hospital, Chengdu, Sichuan, People's Republic of China
[2] School of Foreign Languages, Chengdu University of Information Technology, Chengdu, Sichuan, People's Republic of China

Hamostaseologie 2023;43:271–280.

Address for correspondence Dr. Tongqing Gu, MM, School of Foreign Languages, Chengdu University of Information Technology, No. 24 Block 1, Xuefu Road, Chengdu, 610225, Sichuan, People's Republic of China (e-mail: GuTongqing7706@163.com).

Dr. Jun Zhang, MD, Department of Cardiology, Chengdu First People's Hospital, No. 18, Wanxiang North Road, High-tech Zone, Chengdu, 610016, Sichuan, People's Republic of China (e-mail: Zhangjun1241@outlook.com).

Abstract

Objective Evidence has shown that microRNA (miR)-122–5p is a diagnostic biomarker of acute myocardial infarction. Here, we aimed to uncover the functions of miR-122–5p in the pathological process of myocardial ischemia-reperfusion injury (MI/RI).

Methods An MI/RI model was established by left anterior descending coronary artery ligation in mice. The levels of miR-122–5p, suppressor of cytokine signaling-1 (SOCS1), phosphorylation of Janus kinase 2 (p-JAK2), and signal transducers and activators of transcription (p-STAT3) in the myocardial tissues of mice were measured. Downregulated miR-122–5p or upregulated SOCS1 recombinant adenovirus vectors were injected into mice before MI/RI modeling. The cardiac function, inflammatory response, myocardial infarction area, pathological damage, and cardiomyocyte apoptosis in the myocardial tissues of mice were evaluated. Cardiomyocytes were subjected to hypoxia/reoxygenation (H/R) injury and cardiomyocyte biological function was tested upon transfection of miR-122–5p inhibitor. The target relation between miR-122–5p and SOCS1 was evaluated.

Results miR-122–5p expression and p-JAK2 and p-STAT3 expression were high, and SOCS1 expression was low in the myocardial tissues of MI/RI mice. Decreasing miR-122–5p or increasing SOCS1 expression inactivated the JAK2/STAT3 pathway to alleviate MI/RI by improving cardiac function and reducing inflammatory reaction, myocardial infarction area, pathological damage, and cardiomyocyte apoptosis in mice. Silencing of SOCS1 reversed depleted miR-122–5p-induced cardioprotection for MI/RI mice. In vitro experiments revealed that the downregulation of miR-122–5p induced proliferative, migratory, and invasive capabilities of H/R cardiomyocytes while inhibiting apoptosis. Mechanically, SOCS1 was a target gene of miR-122–5p.

Conclusion Our study summarizes that inhibition of miR-122–5p induces SOCS1 expression, thereby relieving MI/RI in mice.

Keywords

- myocardial ischemia reperfusion injury
- microRNA-122–5p
- suppressor of cytokine signaling-1
- Janus kinase 2/STAT3
- cardiomyocyte
- inflammation
- cardiac function

Introduction

Myocardial ischemia is characterized by a rapid recovery of physiological pH value, $Ca2^{+}$ overload, and depletion of ATP, causing the production of reactive oxygen species, the release of proinflammatory factors, and the invasion of neutrophils.[1] Restoring the blood flow of the ischemic

received
August 26, 2022
accepted after revision
January 11, 2023

Georg Thieme Verlag KG,
Rüdigerstraße 14,
70469 Stuttgart, Germany

DOI https://doi.org/10.1055/a-2013-0336.
ISSN 0720-9355.

myocardium within the first hour after the symptoms appear has become the standard treatment, but the reperfusion process can also induce myocardial injury, which is called myocardial ischemia-reperfusion injury (MI/RI).[2] Non-pharmacological intervention (ischemic pre-conditioning and post-conditioning) and pharmacological intervention (cyclosporine-A, metoprolol, glucose modulators, and abciximab) have been advanced for the treatment of reperfusion injury.[3] Investigations into the underlying mechanism of MI/RI could further facilitate the development of intervention options.

It is widely accepted that modification of microRNAs (miR, small noncoding single-stranded RNA molecules) by pharmacological methods may confer an alternative method for protection against MI/RI.[4] As reported, miR-122–5p is highly expressed in patients with unstable coronary artery disease and stable coronary artery disease.[5] The increased miR-21–5p level is associated with 90-day all-cause mortality of patients with cardiogenic shock,[6] and higher plasma miR-122–5p might be a diagnostic biomarker of acute myocardial infarction (AMI).[7] A miR profile analysis has suggested the pro-apoptotic property of rno-miR-122–5p in post-infarction heart failure,[8] and Lin and Zheng described that inhibition of miR-122–5p impedes apoptosis of cardiomyocytes after myocardial infarction.[9] Induction of the suppressor of cytokine signaling-1 (SOCS1) has shown a protective impact on MI/RI in the liver[10] and intestine.[11] SOCS1 is a negative regulator of pro-inflammatory cytokine signaling, and SOCS1 DNA administration could suppress the inflammatory response in autoimmune myocarditis.[12] Eisenhardt et al stated that SOCS1 could restrain MI/RI-induced inflammatory response and tissue damage in a reactive oxygen species-dependent manner.[13] It is reported that the induction of SOCS1 reduces hippocampal neuronal apoptosis through blocking the Janus kinase 2 (JAK2)/signal transducers and activators of transcription (STAT3) pathway.[14] The activation of the JAK2/STAT3 pathway is suggested to be possibly associated with inflammatory responses and apoptosis in MI/RI.[15] Consulted on the former articles, the mechanism related to the miR-122–5p-mediated SOCS1/JAK2/STAT3 pathway remains an unsolved issue in MI/RI. Here, we initiated this study with a hypothesis that miR-122–5p aggravates MI/RI through inhibition of SOCS1 and activation of the JAK2/STAT3 pathway.

Methods and Materials

Experimental Subjects

A total of 70 healthy C57BL/6J male mice, 6 to 8 weeks old, with a weight of 18 to 22 g, were housed at 22 ± 2 °C. Mice were free to eat and drink with a 12-hour night/dark cycle.

Establishment of an MI/RI Model

The MI/RI model was established by the ligation of the left anterior descending coronary artery with ischemia and reperfusion. In brief, the mice were anesthetized by injection of pentobarbital sodium at 30 mg/kg and connected to the electrocardiograph (Beneheart R3; Mindray, Shenzhen, China). Using the rodent respirator (Techman, Chengdu, China), tracheal intubation and indoor oxygen manual ventilation were performed. The rectal temperature was monitored and maintained between 36 and 37 °C. After thoracotomy at the third rib, the left anterior descending coronary artery was ligated by an 8–0 noninvasive suture (Ethicon, Somerville, New Jersey, United States). Ischemia was confirmed by ST segment-elevated electrocardiogram. After 20 to 30 minutes of ligation, the suture was removed for 60-minute reperfusion. For analgesia, buprenorphine was administered at 0.1 mg/kg. Sham-operated mice underwent the same procedure of the MI/RI model without any coronary artery ligation.[16]

Animal Grouping and Treatment

Mice were randomly divided into seven groups ($n = 10$): the sham group, the MI/RI group, the MI/RI + anti-negative control (NC) group, the MI/RI + anti-miR-122–5p group, the MI/RI + overexpression (oe)-NC group, the MI/RI + oe-SOCS1 group, the MI/RI + anti-miR-122–5p + short hairpin RNA (sh)-NC group, and the MI/RI + anti-miR-122–5p + sh-SOCS1 group. After anesthesia, the mice were injected with recombinant adenoviruses vectors from the left ventricle vertex to the aortic root. Thereafter, the pulmonary artery was clamped to relocate the heart, and the chest was sutured. After 5 days of adenovirus injection, mice ($n = 10$/group) were subjected to MI/RI by left anterior descending coronary artery ligation. Adenoviral vectors containing inhibitor NC, miR-122–5p inhibitor, oe-NC, oe-SOCS1, sh-NC, and sh-SOCS1 were all provided by GeneChem (Shanghai, China). The injection dose of adenovirus was 2×10^{11} pfu/mL.[17]

Echocardiography

Echocardiography was performed using a digital small animal ultrasound system (Vevo 2100 Imaging System; VisualSonics, Toronto, Canada). Left ventricular end-diastolic diameter (LVEDD), left ventricular end-systolic diameter (LVESD), left ventricular ejection fraction (LVEF), left ventricular fractional shortening (LVFS), left ventricular systolic pressure (LVSP), left ventricular end-diastolic pressure (LVEDP), and maximum increase/decrease in left ventricular pressure ($\pm dp/dt_{max}$) were measured.

Determination of Cytokines

After 1 day of ischemia/reperfusion surgery, peripheral blood was collected from the mice in each group. Blood levels of brain natriuretic peptide (BNP; H166, Nanjing Jiancheng Bioengineering Institute) were tested using kits following the manufacturer's instructions. Next, the mice were euthanized; the ischemic myocardial tissue samples were homogenized and centrifuged for the collection of the supernatant; and the levels of interleukin (IL)-1β (H002), IL-6 (H007), and tumor necrosis factor-α (TNF-α, H052) (all from Nanjing Jiancheng Bioengineering Institute) were assessed using kits.[18,19]

Triphenyltetrazolium Chloride Staining

Infarct size was determined by triphenyltetrazolium chloride (TTC) staining. Briefly, the mice (three mice in each

group) were euthanized, and the hearts of the mice were removed and then sliced into 2-mm-thick sections perpendicular to the long axis. After that, the sections were cultivated for 15 minutes at 37 °C with 1% TTC solution (Sigma) in a phosphate solution. The areas of infarcted tissues (TTC-negative staining area) and the whole left ventricle were evaluated by computer morphometry using Bioquant imaging software.[20]

Hematoxylin–Eosin Staining

Myocardial tissue samples of mice were fixed in 4% polyformaldehyde, dehydrated, embedded in paraffin, and sliced (4 µm). After hematoxylin–eosin staining, the slices were observed under a light microscope.[21]

Transferase-Mediated Deoxyuridine Triphosphate-Biotin Nick End Labeling Staining

Transferase-mediated deoxyuridine triphosphate-biotin nick end labeling (TUNEL) staining was performed using a One-step TUNEL Apoptosis Assay Kit (Beyotime Biotechnology, Shanghai, China, C1086) following the manufacturer's instructions, with apoptotic cells exhibiting green nuclear fluorescence.[22]

RNA Immunoprecipitation Assay

RNA immunoprecipitation (RIP) was performed using the EZ-MAGNA RIP kit (Millipore, Massachusetts, United States). Cells were cleaved in RIP lysis buffer and incubated with RIP buffer containing anti-Ago2 (1:20; Abcam, California, United States) or IgG antibody. Subsequently, the protein and RNA complexes were precipitated by magnetic protein A/G beads and centrifuged at 12,000 *g*. After purification by protease K, RNA samples were analyzed by reverse transcription quantitative polymerase chain reaction (RT-qPCR).[23]

RT-qPCR

Total RNAs of ischemic myocardial tissues were extracted with Trizol Reagent (Invitrogen, California, United States). cDNA was obtained using the PrimeScript II First Strand cDNA Synthesis kit (Takara, Dalian, China) and the One-step PrimeScript miRNA cDNA Synthesis kit (Takara). The primers (►**Supplementary Table S1**, online only) were synthesized by Ribobio (Guangzhou, China). SYBR Premix Ex Taq kit (Takara) was used for RT-qPCR. Analyzed by the $2^{-\Delta\Delta CT}$ method, the level of miR-122–5p was standardized to U6, and that of SOCS1 to glyceraldehyde-3-phosphate dehydrogenase (GAPDH).[17]

Western Blot Assay

Ischemic myocardial tissue samples were ice-lysed in lysis buffer (CST, Massachusetts, United States). After the determination of protein concentration using the Bradford method (BioRad, California, United States), the protein sample was separated using sodium dodecyl sulfate polyacrylamide gel electrophoresis and transferred onto polyvinylidene fluoride membranes. Following blocking with 5% skimmed milk or 5% bovine serum albumin (BSA) for 1 hour at ambient temperature, the membrane was probed with diluted primary antibodies to SOCS1 (1:1,000), GAPDH (1:500), phosphorylated (p)-JAK2 (1: 2,000), and p-STAT3 (1:2,000, all from Abcam) overnight at 4 °C. The protein membrane was developed in an enhanced chemiluminescence system (Thermo Fisher Scientific, Massachusetts, United States) after incubation with the secondary antibodies.[24]

Dual Luciferase Reporter Gene Assay

The wild type (WT) or mutated type (MUT) 3′-untranslated region (UTR) of SOCS1 was amplified and cloned into the pGL3-Basic Luciferase Vector (GenePharma, Shanghai, China). The WT SOCS1 3′-UTR and MUT SOCS1 3′-UTR reporters, along with mimic NC and miR-122–5p mimic (GenePharma), were transfected into HL-1 cells (Yajie Biotechnology Co., Ltd., Shanghai, China) using Lipofectamine 3000 (Life Technologies Corporation, Carlsbad, California, United States). Cells were lysed at 48 hours post-transfection and subjected to detection using luciferase detection kit (Biovision, Milpitas, California, United State) and analysis in the luciferase reporter system (Promega, Wisconsin, United States).[25]

Cell Culture, Grouping, Transfection, and Modeling

HL-1 cell lines (ATCC, USA) were cultivated for 48 hours in DMEM containing 10% FBS and 100 mg/L myocilin under the condition of 37 °C and 5% CO_2. When the cells proliferated well, the original medium of HL-1 cells was replaced with hypoxic fluid (DMEM without glucose and serum, prefilled with 1% O_2, 5% CO_2, and 94% N_2). In a closed incubator with 1% O_2, 5% CO_2, and 94% N_2, the cells were cultured at 37 °C for 6-hour hypoxia. Subsequently, the hypoxic fluid was replaced with a glucose-containing oxygen-rich solution prefilled with 5% CO_2, and 95% O_2 (DMEM with 10% FBS), and the cells were cultivated at 37 °C in a closed incubator containing 5% CO_2 and 95% O_2 for 24 hours to develop the hypoxia/reoxygenation (H/R) model. The cells were digested with trypsin, $\sim 10^6$ cells were seeded in 12-well plates, and the serum-free DMEM was further incubated overnight. When the cell confluence reached ~70%, miR-122–5p inhibitor and its NC (GenePharma) at 50 nmol/L were transfected into HL-1 cells by Lipofectamine 2000. Cells were incubated at 37 °C with 5% CO_2 for 6 hours and replaced with fresh DMEM containing 10% FBS and further incubated for another 48 hours. Cells were then modeled for H/R following the steps described earlier.[26]

CCK-8 Assay

The CCK-8 assay was implemented with a commercial kit (Dojindo, Kumamoto, Japan) following the manufacturer's requirements. In short, 100 µL of a suspension with 10^3 cells was appended to each well of a 96-well plate. Upon treatment for 24, 48, and 72 hours, the CCK-8 solution (10 µL) was supplemented to each well. The measurement of cell viability was completed according to the absorbance at 490 nm.

Flow Cytometry

At 48 hours of transfection, cells were digested and harvested in flow tubes, followed by centrifugation for the removal of the supernatant. The Annexin-V-FITC, PI, and HEPES buffer solutions were prepared to the Annexin-V-FITC/PI dye

solution at a ratio of 1:2:50 using the Annexin-V-FITC cell apoptosis detection kit (Biovision). Next, the cells (10^6) were resuspended per 100 µL dye solution, and then cultivated at room temperature for 15 minutes with 1 mL HEPES buffer solution. The fluorescence of FITC and PI was evaluated by exciting 525 and 620 nm band-pass filters with 488 nm wavelength, and the apoptosis was detected.[27]

Transwell Assay

Cell migratory and invasive capabilities were assessed using the Transwell assay (with or without Matrigel). *Cell migration assay*: the transfected cells (200 µL, 5×10^4 cells/mL) were seeded onto the upper chamber of the transfected wells. Upon 24 hours of culture, the cells that migrated to the lower chamber were stained with Giemsa. *Cell invasion assay*: the transfected cells (200 µL, 5×10^4 cells/mL) were seeded onto the Matrigel-coated Transwell upper chamber using Matrigel-precoated Transwell chamber (Corning). Upon 24 hours of culture, the cells retained in the lower half were stained with Giemsa. Images were acquired using a DMI4000B microscope (Leica, Wetzlar, Germany), and cells were counted in five randomly selected fields of view.[28,29]

Statistical Analysis

Statistical analysis was performed using SPSS 20.0 software (IBM, Armonk, New York, United States) and GraphPad Prism 6 (GraphPad Software, La Jolla, California, United States) software. All data were represented by mean ± standard deviation. The normality of the data was checked by the Shapiro–Wilk method. The comparison between the two groups was assessed by unpaired *t*-test, and that among multi-groups by one-way variance analysis and Tukey's multiple comparison test. $p < 0.05$ was considered statistically significant.

Results

Successful Establishment of MI/RI Models in Mice

A mouse MI/RI model was induced, and cardiac function was monitored. The findings implied that after MI/RI modeling, LVEDD, LVESD, and LVEDP were increased, whereas LVEF, LVFS, LVSP, and $\pm dp/dt_{max}$ were reduced in mice (►Fig. 1A). The concentration of inflammatory factors (TNF-α, IL-1β, and IL-6) and BNP was increased in mice after MI/RI modeling (►Fig. 1B). TTC staining showed that myocardial infarction area was increased in MI/RI mice (►Fig. 1C). HE staining exhibited that for sham-operated mice, the myocardial fibers were arranged in bundles with a clear structure without cardiomyocyte edema or inflammatory cell infiltration in the myocardial interstitium. For MI/RI mice, the structure of myocardial fibers was destroyed and disordered; cardiomyocyte local degeneration, rupture, and edema, as well as

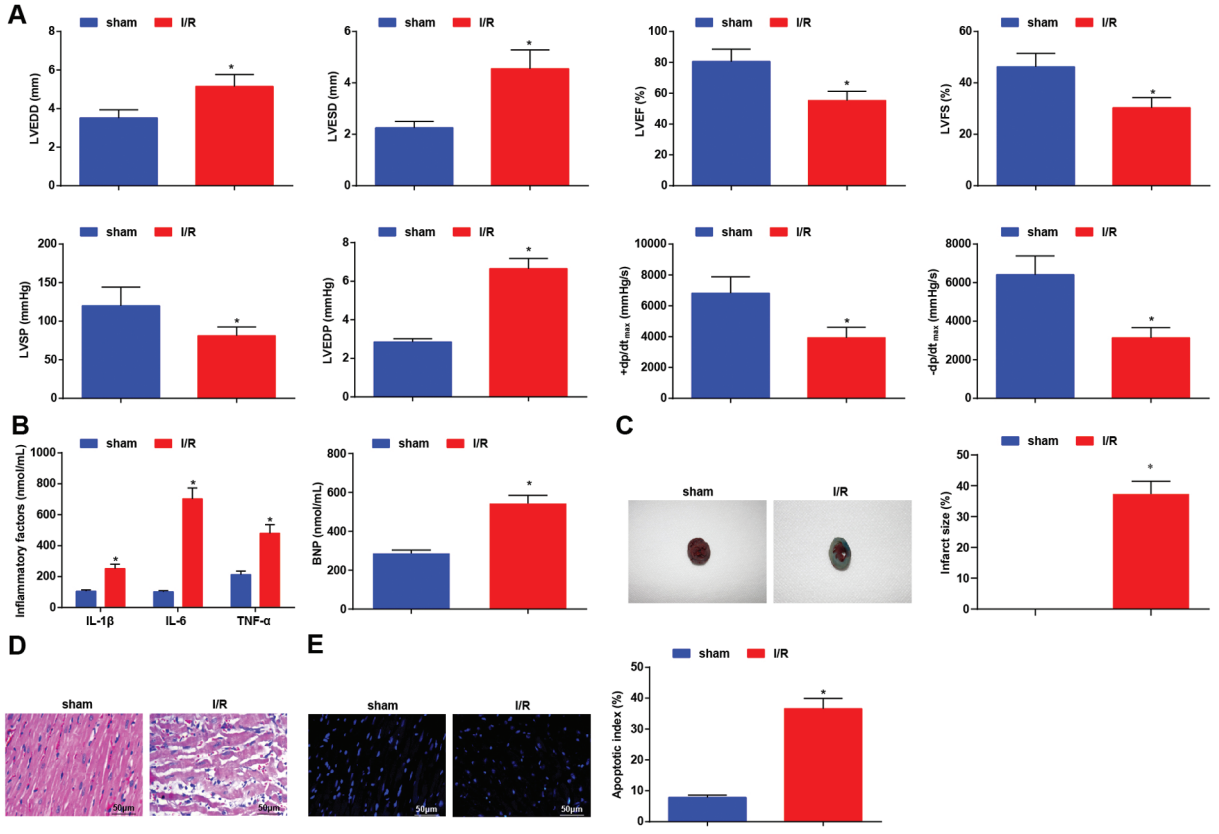

Fig. 1 Successful establishment of a MI/RI model in mice. (**A**) LVEDD, LVESD, LVEF, LVFS, LVSP, LVEDP, and $\pm dp/dt_{max}$ in mice after MI/RI modeling. (**B**) Levels of inflammatory factors (IL-1β, IL-6, and TNF-α) and BNP in mice after MI/RI modeling. (**C**) Myocardial infarction area in mice after MI/RI modeling. (**D**) Pathological damage in mice after MI/RI modeling. (**E**) Cardiomyocyte apoptosis in mice after MI/RI modeling; data were represented by mean ± standard deviation. $^*p < 0.05$ versus the sham group.

inflammatory cell infiltration, were seen (►Fig. 1D). TUNEL staining presented that MI/RI mice had increased cell apoptosis rate in the myocardial tissues (►Fig. 1E). These experimental results confirmed the successful induction of MI/RI in mice.

Depleting miR-122–5p Alleviates MI/RI in Mice and Suppresses Cardiomyocyte Apoptosis In Vitro

As previously described, miR-122–5p is highly expressed in AMI.[7] In mice with MI/RI, it was indicated by RT-qPCR that miR-122–5p was upregulated in the myocardial tissues (►Fig. 2A). Aiming at exploring the actions of miR-122–5p in MI/RI mice, adenoviral anti-miR-122–5p was injected, which successfully suppressed miR-122–5p expression in the myocardial tissues of MI/RI mice (►Fig. 2A). On this account, MI/RI-induced cardiac dysfunction and inflammatory response were alleviated by inhibiting miR-122–5p in MI/RI mice (►Fig. 2B, C). Moreover, the myocardial infarction area, the destruction of myocardial fiber structures, and cardiomyocyte apoptosis were reduced by inhibiting miR-122–5p in MI/RI mice (►Fig. 2D–F).

HL-1 cells were transfected in vitro with miR-122–5p inhibitor and successful transfection was confirmed by RT-qPCR assay (►Fig. 3A). CCK-8 assay, Transwell assay, and flow cytometry were implemented to examine cardiomyocyte biological function after interfering with miR-122–5p. The results disclosed that the downregulation of miR-122–5p induced proliferative, migratory, and invasive capabilities while inhibiting apoptosis in H/R cardiomyocytes (►Fig. 3B–D).

All in all, miR-122–5p downregulation alleviated MI/RI in mice and suppressed cardiomyocyte apoptosis in vitro.

SOCS1 Is Targeted by miR-122–5p

The specific binding site was found between SOCS1 and miR-122–5p by the online analysis Web site Starbase (►Fig. 4A). Furthermore, luciferase activity and RIP assay were implemented to verify the target relationship between miR-122–5p and SOCS1. The findings demonstrated that the luciferase activity of WT SOCS1 3′-UTR was diminished in cells by miR-122–5p mimic (►Fig. 4B); miR-122–5p and SOCS1 were highly immunoprecipitated by Ago2 (►Fig. 4C).

After the treatment of adenoviral anti-miR-122–5p, SOCS1 levels were elevated (►Fig. 4D–F). In summary, miR-122–5p can negatively modulate SOCS1.

Inducing SOCS1 Expression Alleviates MI/RI in Mice

Measurement of SOCS1 expression in the myocardial tissues of MI/RI mice was conducted using RT-qPCR and Western blot, and the results highlighted that SOCS1 levels were lowered after MI/RI modeling (►Fig. 5A). Next, for a better understanding of the role of SOCS1 in MI/RI mice, oe-NC or oe-SOCS1 adenovirus was introduced into mice, and the results suggested that oe-SOCS1 treatment elevated SOCS1 expression in the myocardial tissues of MI/RI mice (►Fig. 5B). It was experimentally observed that upregulation of SOCS1

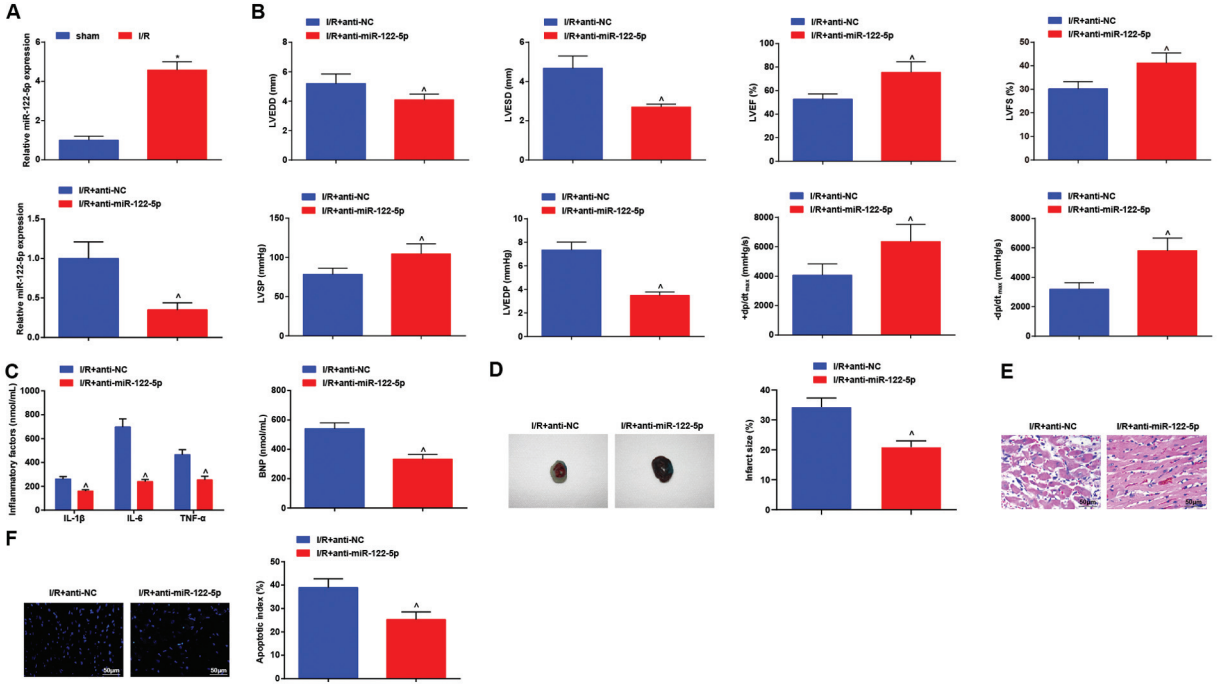

Fig. 2 Depleting miR-122–5p alleviates MI/RI in mice. (**A**) miR-122–5p expression level in mice after MI/RI modeling and in MI/RI mice after injection with anti-miR-122–5p. (**B**) LVEDD, LVESD, LVEF, LVFS, LVSP, LVEDP, and $\pm dp/dt_{max}$ in mice after injection with anti-miR-122–5p. (**C**) Levels of inflammatory factors (IL-1β, IL-6, and TNF-α) and BNP in mice after injection with anti-miR-122–5p. (**D**) Myocardial infarction area in MI/RI mice after injection with anti-miR-122–5p. (**E**) Pathological damage in MI/RI mice after injection with anti-miR-122–5p. (**F**) Cardiomyocyte apoptosis in MI/RI mice after injection with anti-miR-122–5p; data were represented by mean ± standard deviation. $^{*}p < 0.05$ versus the sham group; $^{\wedge}p < 0.05$ versus the I/R + anti-NC group.

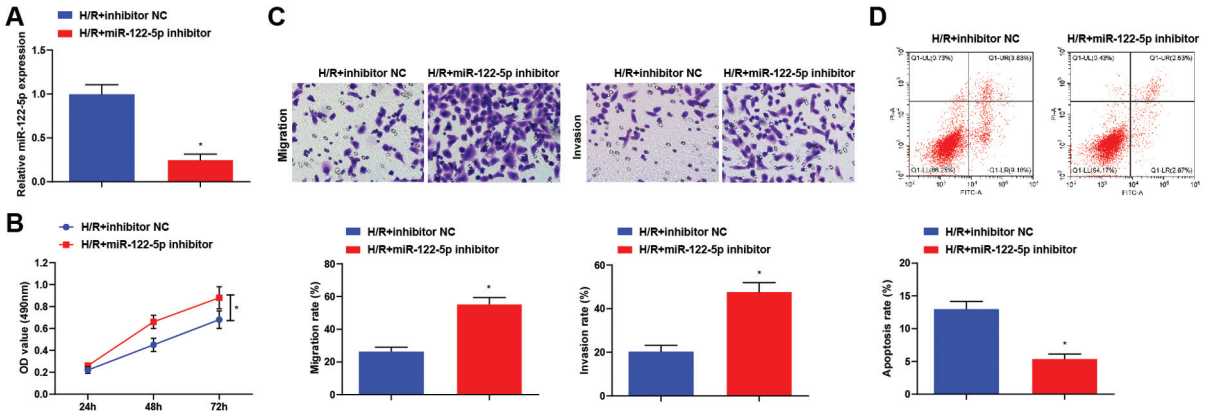

Fig. 3 Depleting miR-122–5p suppresses H/R cardiomyocyte apoptosis in vitro. (**A**) The miR-122–5p transfection efficiency of cardiomyocytes was determined by RT-qPCR experiment. (**B**) Cell proliferative capacity was measured by CCK-8 assay. (**C**) Transwell assay for the evaluation of cell migration and invasion (**D**) Cell apoptosis rate was measured by flow cytometry; data were represented by mean ± standard deviation. $^{*}p < 0.05$ versus the H/R + inhibitor NC group.

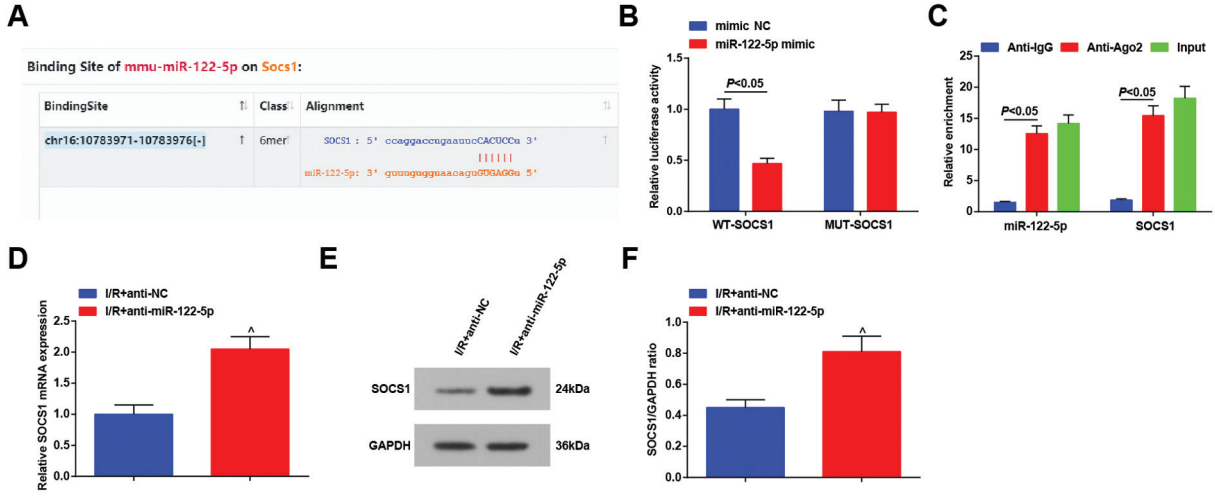

Fig. 4 SOCS1 is targeted by miR-122–5p. (**A**) The binding site of miR-122–5p and SOCS1 on Starbase. (**B, C**) The binding relation of miR-122–5p and SOCS1 was verified by luciferase activity assay and RIP assay. (**D–F**) SOCS1 mRNA and protein expression in MI/RI mice after injection with anti-miR-122–5p; data were represented by mean ± standard deviation. $^{\wedge}p < 0.05$ versus the I/R + anti-NC group.

by oe-SOCS1 adenovirus induced cardiac function recovery, in concert with reduction of myocardial infarction area, inflammation, pathological damage, and cardiomyocyte apoptosis (►Fig. 5C–G).

Silencing of SOCS1 Reverses Depleted miR-122–5p-Induced Cardioprotection for MI/RI Mice

The mechanism of the miR-122–5p/SOCS1 axis on MI/RI was further assessed, and the anti-miR-122–5p + sh-NC group and the anti-miR-122–5p + sh-SOCS1 group were set. RT-qPCR and Western blot confirmed the reduction of SOCS1 expression mediated by anti-miR-122–5p + sh-SOCS1 in comparison to anti-miR-122–5p + sh-NC (►Fig. 6A). We then performed functional assays on the treated mice and showed that silencing of SOCS1 reversed the effects of miR-122–5p downregulation on myocardial tissues in MI/RI mice (►Fig. 6B–F).

Downregulation of miR-122–5p Inactivates the JAK2/STAT3 Pathway through Elevating SOCS1 Expression

p-JAK2 and p-STAT3 levels were determined by Western blot analysis. The results displayed that p-JAK2 and p-STAT3 levels were high in the myocardial tissues of MI/RI mice. The decrease of p-JAK2 and p-STAT3 levels was seen in MI/RI mice after injection with adenoviral anti-miR-122–5p or oe-SOCS1 (►Fig. 7A, B).

Discussion

MI/RI is the main pathological manifestation of coronary artery disease (CAD), with a relatively high incidence. In a mouse model of MI/RI, the miR-122–5p-related mechanism was deciphered in this present study, and the findings demonstrated that downregulation of miR-122–5p

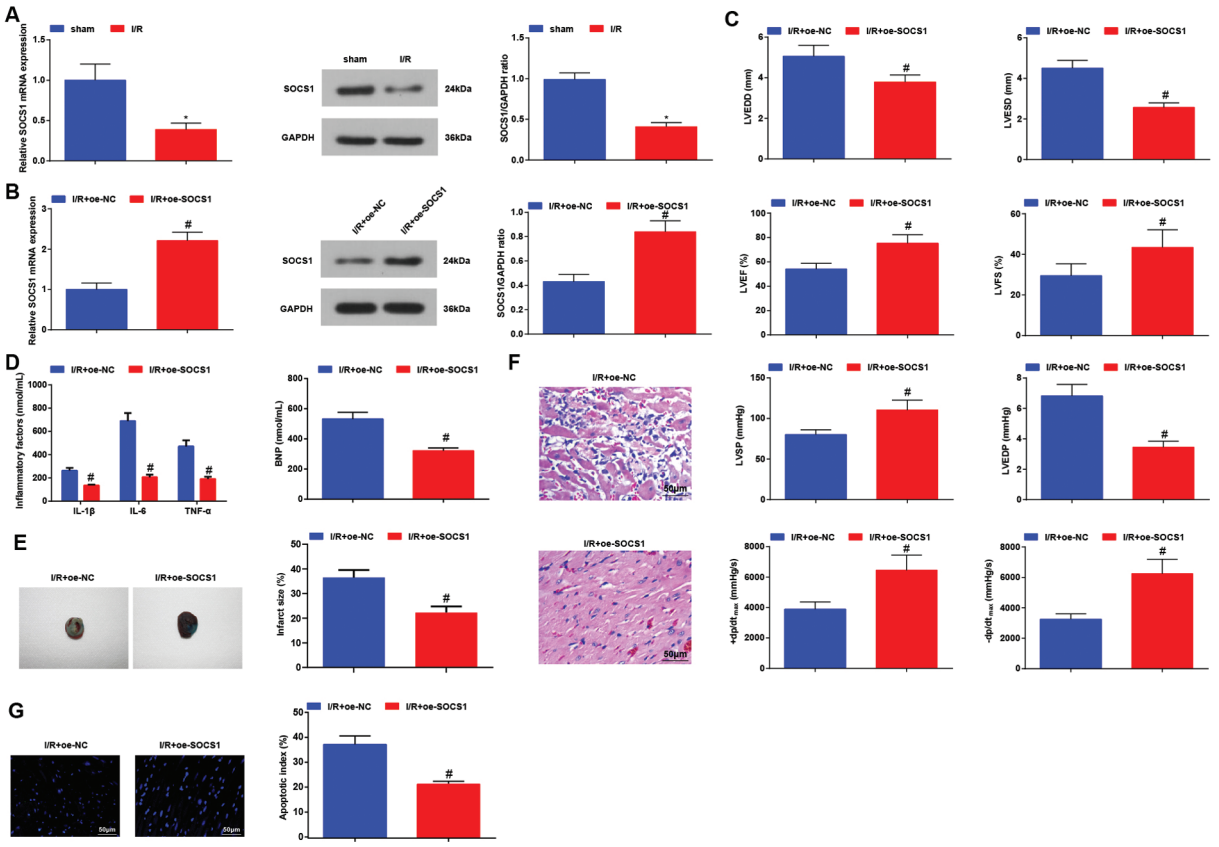

Fig. 5 Inducing SOCS1 expression alleviates MI/RI in mice. (**A, B**) SOCS1 mRNA and protein expression in mice after MI/RI modeling. (**C**) LVEDD, LVESD, LVEF, LVFS, LVSP, LVEDP, and $\pm dp/dt_{max}$ in MI/RI mice after injection with oe-SOCS1 adenovirus. (**D**) Levels of inflammatory factors (IL-1β, IL-6, and TNF-α) and BNP in MI/RI mice after injection with oe-SOCS1 adenovirus. (**E**) Myocardial infarction area in MI/RI mice after injection with oe-SOCS1 adenovirus. (**F**) Pathological damage in MI/RI mice after injection with oe-SOCS1 adenovirus. (**G**) Cardiomyocyte apoptosis in MI/RI mice after injection with oe-SOCS1 adenovirus; data were represented by mean ± standard deviation. $^{*}p < 0.05$ versus the sham group; $^{\#}p < 0.05$ versus the I/R + oe-NC group.

attenuated the pathogenic responses of MI/RI by inducing SOCS1 expression and inactivating the JAK2/STAT3 pathway.

Initially, miR-122–5p expression was found to be elevated in the myocardial tissues of MI/RI mice. Correspondingly, the increased miR-122–5p expression has been observed in the serum of patients with CAD[5] or with AMI.[30] With the aim to probe the miR-122–5p-mediated process of MI/RI, miR-122–5p expression intervention was performed, which acted to improve cardiac function (shown with decreased LVEDD, LVESD, and LVEDP, and increased LVEF, LVFS, LVSP, and $\pm dp/dt_{max}$), repress inflammatory response (evident by inhibited TNF-α, IL-1β, and IL-6 levels), and decrease the damage of myocardium and apoptosis of cardiomyocytes. Also, it is noted that cardiomyocytes overexpressing miR-122–5p exhibit an augmented apoptosis rate and diminished cell viability.[9] Elevating miR-122–5p expression in hypoxia-conditioned cardiomyocytes elevates cellular apoptosis and disturbs cell activities.[31] Concerning the action of miR-122–5p in heart diseases, Song et al have supported that sepsis-induced myocardial injury, including inflammatory cell infiltration, inflammation, and apoptosis, could be attenuated by reduction of miR-122–5p.[32] Regarding an article proposed by Yang et al, depression of miR-122–5p mitigates drug-induced liver injury in part by restraining apoptosis of normal liver cells, whereas promotion of miR-122–5p exhibits the opposite outcome.[33] Lately, a publication has highlighted that silenced miR-122–5p suppresses inflammatory response in mice with acute lung injury, as well as blocks apoptosis of injured lung microvascular endothelial cells.[34] Importantly, the proapoptotic phenotype miR-122–5p has been reflected in kidney injury, and the knockdown of miR-122–5p could decrease cadmium-induced kidney injury in a cell model.[35]

Afterward, miR-122–5p-targeted SOCS1 attracted the research interest. Lowly expressed SOCS1 was determined in MI/RI mice; elevation of SOCS1 expression induced cardioprotection for MI/RI mice, but a reduction of SOCS1 reversed the depleted miR-122–5p-induced impacts on MI/RI mice. Indeed, SOCS1 expression is lowered by myocardial infarction, and SOCS1 silencing increases the recruitment of inflammatory cells.[13] The anti-inflammation activity of SOCS1 has been widely reported, such as in hyperoxic acute lung injury to reduce infiltration of inflammatory cells.[36] In the process of ischemic preconditioning, SOCS1 expression is induced to prevent intestinal MI/RI-induced inflammation and apoptosis.[11]

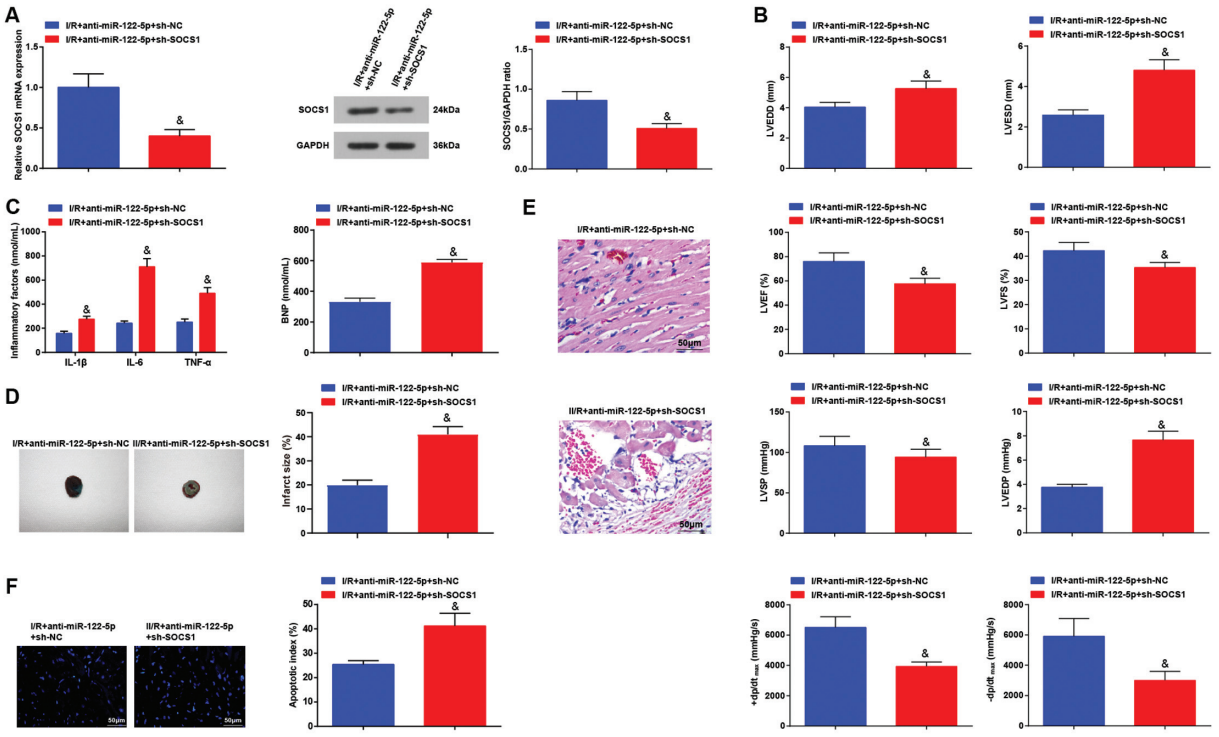

Fig. 6 Silencing of SOCS1 reverses depleted miR-122–5p-induced cardioprotection for MI/RI mice. (**A**) SOCS1 mRNA and protein expression level in MI/RI mice after injection with anti-miR-122–5p and sh-SOCS1. (**B**) LVEDD, LVESD, LVEF, LVFS, LVSP, LVEDP, and $\pm dp/dt_{max}$ in MI/RI mice after injection with anti-miR-122–5p and sh-SOCS1. (**C**) Levels of inflammatory factors (IL-1β, IL-6, and TNF-α) and BNP in MI/RI mice after injection with anti-miR-122–5p and sh-SOCS1. (**D**) Myocardial infarction area in MI/RI mice after injection with anti-miR-122–5p and sh-SOCS1. (**E**) Pathological damage in MI/RI mice after injection with anti-miR-122–5p and sh-SOCS1. (**F**) Cardiomyocyte apoptosis in MI/RI mice after injection with anti-miR-122–5p and sh-SOCS1; data were represented by mean ± standard deviation. $^{\&}p < 0.05$ versus the I/R + anti-miR-122–5p + sh-NC group.

In the end, the JAK2/STAT3 signaling pathway was discovered to be activated during the process of MI/RI, which was blocked by decreasing miR-122–5p or increasing SOCS1. SOCS1 could block the JAK2/STAT3 signaling pathway, thereby inhibiting neuronal apoptosis and inflammation induced by oxygen-glucose deprivation-activated microglia.[14] In fact, p-JAK2 and p-STAT3 expression levels are enhanced in a rat model with MI/RI.[37] Bai et al have estimated that *Corydalis*

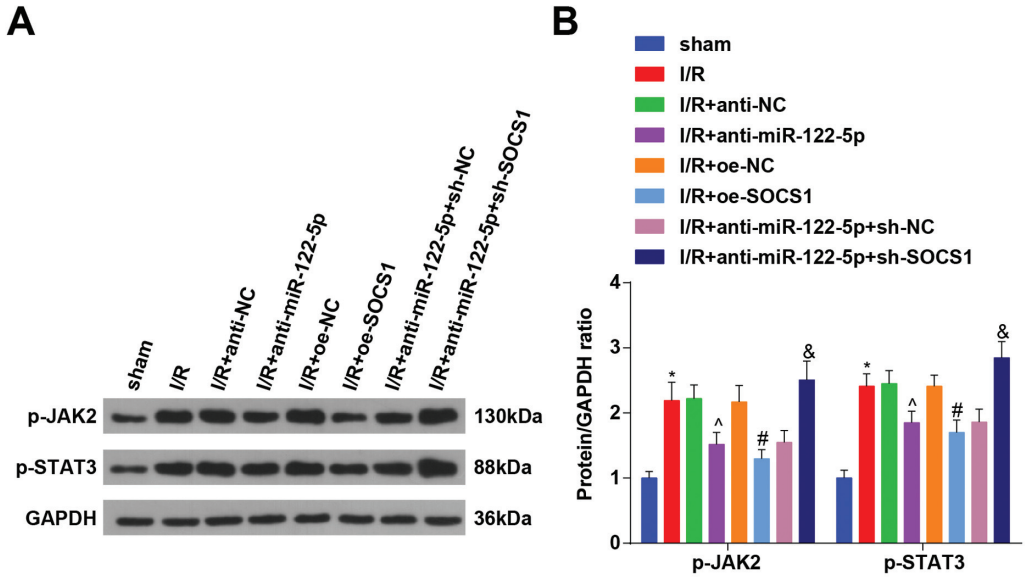

Fig. 7 Downregulated miR-122–5p inactivates the JAK2/STAT3 pathway through increasing SOCS1 expression. (**A, B**) Levels of p-JAK2 and p-STAT3 in MI/RI mice; data were represented by mean ± standard deviation. $^{*}p < 0.05$ versus the sham group; $^{\wedge}p < 0.05$ versus the I/R + anti-NC group; $^{\#}p < 0.05$ versus the I/R + oe-NC group; $^{\&}p < 0.05$ versus the I/R + anti-miR-122–5p + sh-NC group.

hendersonii Hemsl. could protect against myocardial injury by inactivating the JAK2-STAT3 signaling pathway.[38] Coincidentally, another study has analyzed that IL-23 aggravates inflammation and apoptosis in rats with MI/RI partly through inducing the activation of the JAK2/STAT3 signaling pathway.[15] All these investigations confirmed our findings to some extent.

To conclude, this research demonstrates that suppression of miR-122–5p confers cardioprotective benefits for MI/RI mice via upregulating SOCS1 expression. This research may offer a theoretical basis for developing therapeutic agents in the treatment of MI/RI. However, this study assessed only the status of the JAK2/STAT3 signaling pathway in MI/RI, and did not further explore the mechanism of the JAK2/STAT3 signaling pathway in the disease, which is the main limitation requiring further inspection.

Ethical Statement

Experimental approval was signed by the Ethics Committee of Chengdu First People's Hospital. Animal suffering was minimized as much as possible.

Funding

This study was supported by the National Natural Science Foundation of China (no. 81270220).

Conflict of Interest

The authors have no conflicts of interest to declare.

References

1 Frank A, Bonney M, Bonney S, Weitzel L, Koeppen M, Eckle T. Myocardial ischemia reperfusion injury: from basic science to clinical bedside. Semin Cardiothorac Vasc Anesth 2012;16(03): 123–132
2 Wan Ab Naim WN, Mohamed Mokhtarudin MJ, Chan BT, Lim E, Ahmad Bakir A, Nik Mohamed NA. The study of myocardial ischemia-reperfusion treatment through computational modelling. J Theor Biol 2021;509:110527
3 Ibáñez B, Heusch G, Ovize M, Van de Werf F. Evolving therapies for myocardial ischemia/reperfusion injury. J Am Coll Cardiol 2015; 65(14):1454–1471
4 Ye Y, Perez-Polo JR, Qian J, Birnbaum Y. The role of microRNA in modulating myocardial ischemia-reperfusion injury. Physiol Genomics 2011;43(10):534–542
5 Singh S, de Ronde MWJ, Kok MGM, et al. MiR-223-3p and miR-122-5p as circulating biomarkers for plaque instability. Open Heart 2020;7(01):e001223
6 Hänninen M, Jäntti T, Tolppanen H, et al; For The CardShock Study Group. Association of miR-21-5p, miR-122-5p, and miR-320a-3p with 90-Day Mortality in Cardiogenic Shock. Int J Mol Sci 2020;21 (21):7925
7 Wang Y, Chang W, Zhang Y, et al. Circulating miR-22-5p and miR-122-5p are promising novel biomarkers for diagnosis of acute myocardial infarction. J Cell Physiol 2019;234(04):4778–4786
8 Liu X, Meng H, Jiang C, Yang S, Cui F, Yang P. Differential microRNA expression and regulation in the rat model of post-infarction heart failure. PLoS One 2016;11(08):e0160920
9 Lin J, Zheng X. Salvianolate blocks apoptosis during myocardial infarction by down regulating miR-122-5p. Curr Neurovasc Res 2017;14(04):323–329
10 Sano T, Izuishi K, Hossain MA, et al. Protective effect of lipopolysaccharide preconditioning in hepatic ischaemia reperfusion injury. HPB (Oxford) 2010;12(08):538–545
11 Liu SZ, He XM, Zhang X, Zeng FC, Wang F, Zhou XY. Ischemic preconditioning-induced SOCS-1 protects rat intestinal ischemia reperfusion injury via degradation of TRAF6. Dig Dis Sci 2017;62 (01):105–114
12 Tajiri K, Imanaka-Yoshida K, Matsubara A, et al. Suppressor of cytokine signaling 1 DNA administration inhibits inflammatory and pathogenic responses in autoimmune myocarditis. J Immunol 2012;189(04):2043–2053
13 Eisenhardt SU, Weiss JB, Smolka C, et al. MicroRNA-155 aggravates ischemia-reperfusion injury by modulation of inflammatory cell recruitment and the respiratory oxidative burst. Basic Res Cardiol 2015;110(03):32
14 Wang H, Li Z, Gao J, Liao Q. Circular RNA circPTK2 regulates oxygen-glucose deprivation-activated microglia-induced hippocampal neuronal apoptosis via miR-29b-SOCS-1-JAK2/STAT3-IL-1β signaling. Int J Biol Macromol 2019;129:488–496
15 Liao Y, Hu X, Guo X, Zhang B, Xu W, Jiang H. Promoting effects of IL–23 on myocardial ischemia and reperfusion are associated with increased expression of IL–17A and upregulation of the JAK2–STAT3 signaling pathway. Mol Med Rep 2017;16(06):9309–9316
16 Hsu CP, Zhai P, Yamamoto T, et al. Silent information regulator 1 protects the heart from ischemia/reperfusion. Circulation 2010; 122(21):2170–2182
17 Zheng T, Yang J, Zhang J, et al. Downregulated microRNA-327 attenuates oxidative stress-mediated myocardial ischemia reperfusion injury through regulating the FGF10/Akt/Nrf2 signaling pathway. Front Pharmacol 2021;12:669146
18 Ku HC, Chen WP, Su MJ. DPP4 deficiency preserves cardiac function via GLP-1 signaling in rats subjected to myocardial ischemia/reperfusion. Naunyn Schmiedebergs Arch Pharmacol 2011;384(02):197–207
19 Dong W, Yang R, Yang J, et al. Resveratrol pretreatment protects rat hearts from ischemia/reperfusion injury partly via a NALP3 inflammasome pathway. Int J Clin Exp Pathol 2015;8(08): 8731–8741
20 Zhang Y, Li H, Zhao G, et al. Hydrogen sulfide attenuates the recruitment of $CD11b^{+}Gr\text{-}1^{+}$ myeloid cells and regulates Bax/Bcl-2 signaling in myocardial ischemia injury. Sci Rep 2014;4:4774
21 Huang Y, Long X, Li X, Li S, He J. The role of oxymatrine in amelioration of acute lung injury subjected to myocardial I/R by inhibiting endoplasmic reticulum stress in diabetic rats. Evid Based Complement Alternat Med 2020;2020:8836904
22 Zhang J, Shi X, Gao J, et al. Danhong injection and trimetazidine protect cardiomyocytes and enhance calcium handling after myocardial infarction. Evid Based Complement Alternat Med 2021;2021:2480465
23 Zhang Y, Fan X, Yang H. Long noncoding RNA FTX ameliorates hydrogen peroxide-induced cardiomyocyte injury by regulating the miR-150/KLF13 axis. Open Life Sci 2020;15(01):1000–1012
24 Shimada BK, Yorichika N, Higa JK, et al. mTOR-mediated calcium transients affect cardiac function in ex vivo ischemia-reperfusion injury. Physiol Rep 2021;9(06):e14807
25 Wu X, Liu Y, Mo S, Wei W, Ye Z, Su Q. LncRNA TUG1 competitively binds to miR-340 to accelerate myocardial ischemia-reperfusion injury. FASEB J 2021;35(01):e21163
26 Lang Z, Fan X, Lin H, Qiu L, Zhang J, Gao C. Silencing of SNHG6 alleviates hypoxia/reoxygenation-induced cardiomyocyte apoptosis by modulating miR-135a-5p/HIF1AN to activate Shh/Gli1 signalling pathway. J Pharm Pharmacol 2021;73(01):22–31
27 Diaz D, Prieto A, Reyes E, Barcenilla H, Monserrat J, Alvarez-Mon M. Flow cytometry enumeration of apoptotic cancer cells by apoptotic rate. Methods Mol Biol 2015;1219:11–20
28 Huang Y, Yu S, Cao S, et al. MicroRNA-222 promotes invasion and metastasis of papillary thyroid cancer through targeting protein phosphatase 2 regulatory subunit B alpha expression. Thyroid 2018;28(09):1162–1173
29 Qiu K, Xie Q, Jiang S, Lin T. Silencing of DJ-1 reduces proliferation, invasion, and migration of papillary thyroid cancer cells in vitro,

probably by increase of PTEN expression. Int J Clin Exp Pathol 2019;12(06):2046–2055
30 Cortez-Dias N, Costa MC, Carrilho-Ferreira P, et al. Circulating miR-122-5p/miR-133b ratio is a specific early prognostic biomarker in acute myocardial infarction. Circ J 2016;80(10):2183–2191
31 Peng H, Luo Y, Ying Y. lncRNA XIST attenuates hypoxia-induced H9c2 cardiomyocyte injury by targeting the miR-122-5p/FOXP2 axis. Mol Cell Probes 2020;50:101500
32 Song W, Zhang T, Yang N, Zhang T, Wen R, Liu C. Inhibition of micro RNA miR-122-5p prevents lipopolysaccharide-induced myocardial injury by inhibiting oxidative stress, inflammation and apoptosis via targeting GIT1. Bioengineered 2021;12(01): 1902–1915
33 Yang Z, Wu W, Ou P, et al. MiR-122-5p knockdown protects against APAP-mediated liver injury through up-regulating NDRG3. Mol Cell Biochem 2021;476(02):1257–1267
34 Lu Z, Feng H, Shen X, et al. MiR-122-5p protects against acute lung injury via regulation of DUSP4/ERK signaling in pulmonary microvascular endothelial cells. Life Sci 2020;256:117851
35 Yuan W, Liang L, Huang K, et al. MiR-122-5p and miR-326-3p promote cadmium-induced NRK-52E cell apoptosis by down-regulating PLD1. Environ Toxicol 2020;35(12):1334–1342
36 Galam L, Parthasarathy PT, Cho Y, et al. Adenovirus-mediated transfer of the SOCS-1 gene to mouse lung confers protection against hyperoxic acute lung injury. Free Radic Biol Med 2015;84:196–205
37 Zhang Y, Shi K, Lin T, et al. Ganoderic acid A alleviates myocardial ischemia-reperfusion injury in rats by regulating JAK2/STAT3/NF-κB pathway. Int Immunopharmacol 2020;84:106543
38 Bai R, Yin X, Feng X, et al. *Corydalis hendersonii Hemsl.* protects against myocardial injury by attenuating inflammation and fibrosis via NF-κB and JAK2-STAT3 signaling pathways. J Ethnopharmacol 2017;207:174–183

